Spanwise Pressure Measurements of Weak Normal Shock Wave/Turbulent Boundary Layer Interactions in a Supersonic Nozzle

Hong, Jong Woo
Department of Energy Conversion Engineering, Interdisciplinary Graduate School of Engineering Sciences, Kyushu University

Miyazato, Yoshiaki
Department of Energy Conversion Engineering, Interdisciplinary Graduate School of Engineering Sciences, Kyushu University

Matsuo, Kazuyasu
Department of Energy Conversion Engineering, Interdisciplinary Graduate School of Engineering Sciences, Kyushu University

https://doi.org/10.15017/17356

九州大学大学院総合理工学研究科報告
第16巻 第4号 395-405頁 平成7年3月

Engineering Sciences Reports, Kyushu University
(KYUSHU DAIGAKU SOGORIKOGAKU KENKYUKA HOKOKU)
Vol. 16, No. 4, pp. 395 - 405, March. 1995

Spanwise Pressure Measurements of Weak Normal Shock Wave/Turbulent Boundary Layer Interactions in a Supersonic Nozzle

Jong-Woo HONG*, Yoshiaki MIYAZATO** and Kazuyasu MATSUO**

(Received November 15, 1994)

The characteristics of flow field along spanwise direction induced by the interaction of weak normal shock wave with turbulent boundary layer in a supersonic nozzle were investigated experimentally. In the range of just upstream shock Mach number about 1.10 to 1.80, detailed time mean wall static pressure measurements were carried out along spanwise direction using multiple pressure transducers. Also, the relations between variations of upstream boundary layer and behavior of interaction flow fields were investigated. As a result, it is revealed that upstream boundary layer thickness influences the behavior of interaction somewhat for case of well-separated flow. And, another one is revealed that there is some spawise pressure difference in unseparated flow, however, no so much difference is found in well-separated flow case.

1. Introduction

The flow characteristics of shock wave and turbulent boundary layer interaction **(STBLI)** have been investigated by many researchers. Recently, in accordance with elevated importance of application to practical industries, many aircraft designers and workers on site have been urged to understand inherent characteristics about 3-dimensional STBLI phenomenon which occurred in flow field for supersonic inlets of turbojets and ramjets[1], in transonic airfoil flows[2] and in transonic compressor rotor passage[3]. Also its importances were brought to the fore in sphere of wind tunnel test investigation using supersonic nozzle and diffuser flows[4) 5]. As progressing of innovatory developments of experimental apparatuses and flow measuring systems, a few investigators begin to undertake the experimental investigations of three-dimensional STBLI flow fields[6) 7]. Additionally by brilliant development of powerful super-computer with high speed and enormous memory, it becomes possible to investigate this phenomenon numerically to a some extent[8) 9]. However, because its ultimate difficulty and complexity related in measuring methods of flow characteristics have prevented many workers from approaching with ease, almost investigations of STBLI rely on experimental methods using two-dimensional measurements. Almost results[10) 11] of them were concentrated on simple two-dimensional measurement methods along transverse and longitudinal direction to main flow. By mercy of their strong and sticky endeavors, the detailed structures of STBLI phenomenon are qualitatively well understood in two-dimensional view point, however, almost no research

*Department of Energy Conversion Engineering, Graduate Student
**Department of Energy Conversion Engineering

results along spanwise is informed but a few of Reda and his group's[12)-14)]. Therefore, we devised a special experimental apparatus, say, wall static pressure measurable device along both spanwise and streamwise direction. The experimental results of time mean wall static pressure measurement along streamwise had been informed in reference 15. Soon after were informed the results of time fluctuating pressure measurements including a proposal of shock wave oscillation mechanism[16)]. In present paper, as the third of experimental result of a series of investigations, time mean wall static pressure measurements were carried out using specially designed rotatable plug with multiple pressure transducers which supply almost continuous wall static pressure distributions along spanwise and streamwise direction. Additionally the influence of upstream boundary layer thickness variation on flow characteristics in STBLI phenomenon was investigated by using adjustable upstream duct length.

2. Experimental Apparatus

2.1 Supersonic indraft wind tunnel

Fig. 1 is the schematic diagram of intermittent type supersonic indraft wind tunnel used in present investigations at the High Speed Flow Laboratory of Kyushu University. This wind tunnel is roughly consisted of four sections-reservoir tank, test section, settling chamber with volume of $0.3m^3$ and vacuum tank. At first, the reservoir tank whose volume is $18m^3$ is filled with the atmospheric air employed as working fluid which is supplied from the air. In order to prevent condensation phenomenon occurred in which atmospheric air with high relative humidity is undergone rapid expansion process in test section, moisture remover is set up in internal section. Usage of the moisture remover maintains the relatie humidity about 20% below during the tests. If necessary, controlling of the total temperature in reservoir tank is done by electric heater. Also, circulating fan mixes the working fluids uniform. Of course, all flow characteristics in reservoir tank were adjusted to desired state before starting the experiment and monitored in controlling room during the tests. Detailed expressions about test section and settling chamber will be given in section 2.2. The dotted circle in test section indicates the optically measurable scope of flow visualization. The method of flow visualization used in present experiments will be given later in section 2.4. Vacuum tank whose volume is $15m^3$ is connected to vacuum pump with normal capacity of 3000*l*/min. This vacuum pump evacuates the air involved within the vacuum tank and directly exhausts into the atmosphere. In considering of the volume of reservoir tank, vacuum tank and mass flow rate of test section, the steady working time of this wind tunnel is about 60 seconds.

2. 2 Test model

Fig. 2 indicates the detailed disposition of test section, settling chamber, Duct Ⅰ and Duct Ⅱ. Before entering the explanation of test model, the method of changing the flow characteristics in upstream boundary layer is discussed here. One point of being worthy of notice in present experimental device is that it is possible for test section to change its location with Duct Ⅰ or Duct Ⅱ. The test section with 720 mm length is able to change its location by altering the arrangement with Duct Ⅰ and Duct Ⅱ whose length is both 400 mm. All ducts are rectangulars with dimensions of 60 mm height and 38 mm width. For the

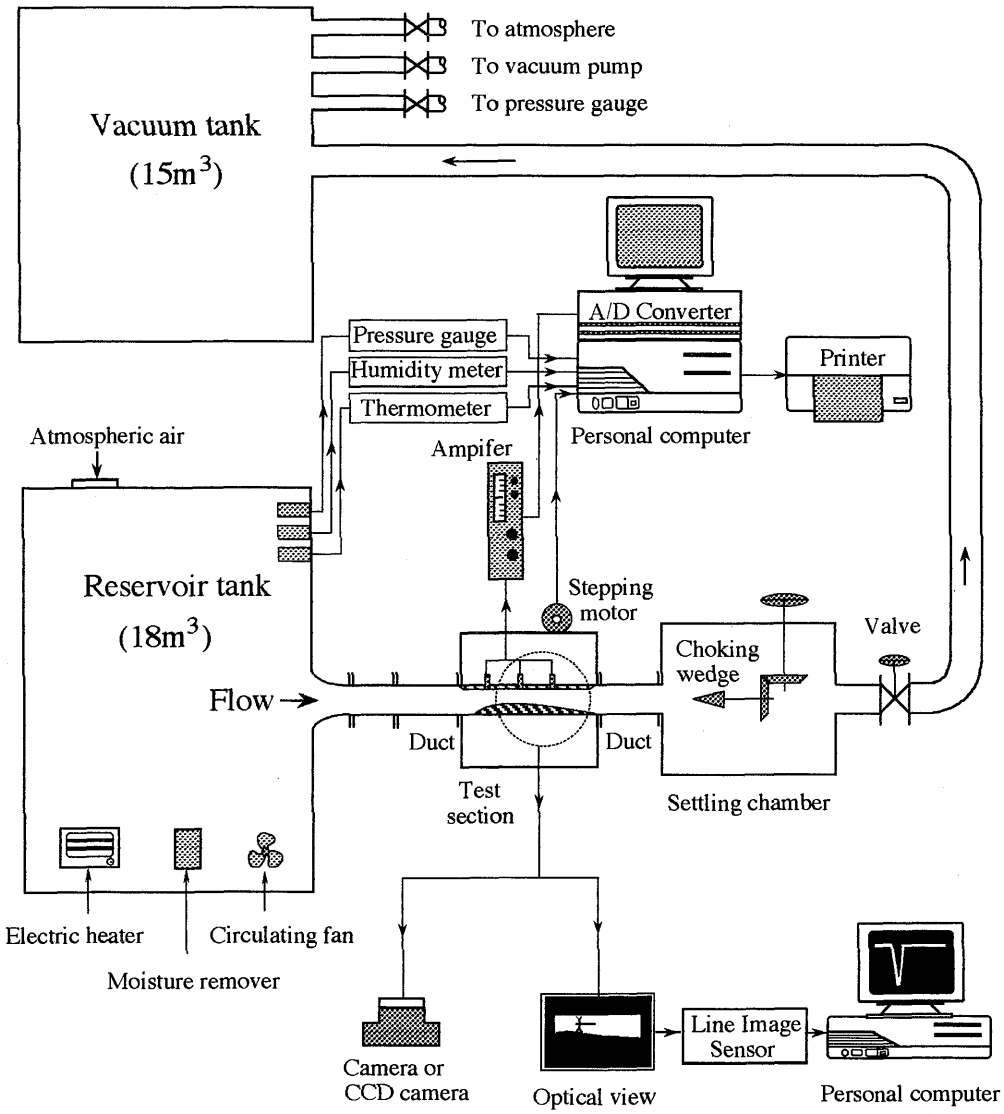

Fig. 1 Schematic diagram of indraft supersonic wind tunnel

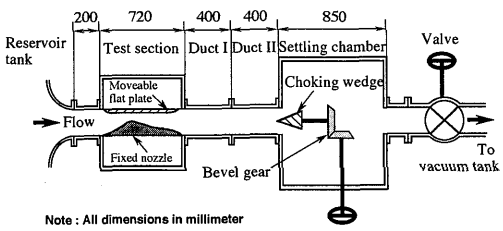

Fig. 2 Details of test section and settling chamber

convenience of explanation, the arrangement as seeing in **Fig. 2**-test section, Duct Ⅰ and Duct Ⅱ in order from reservoir is named to **Test I**. In arrangement of Duct Ⅰ, Duct Ⅱ and test section in order, the case is called to **Test II**. Concludingly speaking, by way of changing the upstream duct length, although its changeable quantity is

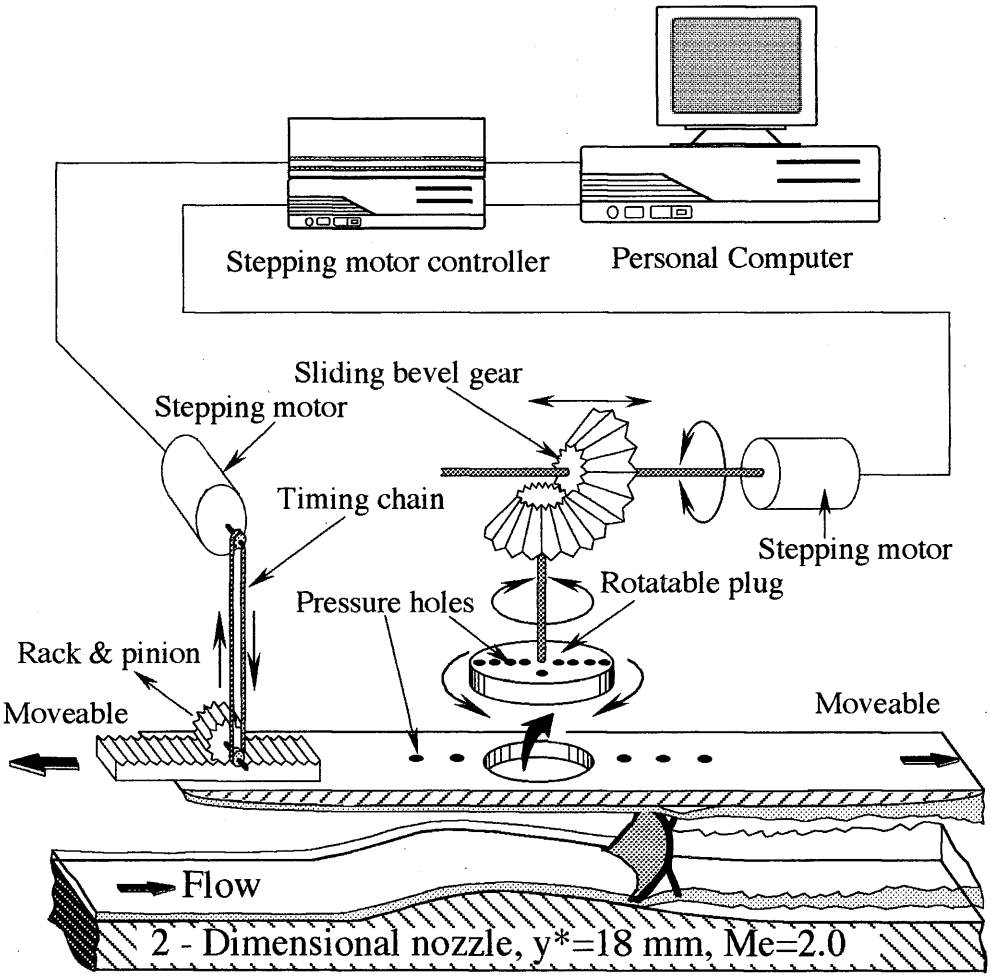

Fig. 3 Schematic sketch of flow field and mechanism of upper wall flat plate

not so much, it is possible to change upstream boundary layer thickness entering interaction region. Its detailed quantitative variations will be explained in section 3.1. Next, the explanations about settling chamber will be given, a choking wedge movable forward and backward along duct center line is set up with a set of bevel gear connected in manual-working handle. The choking wedge which plays a role as the second throat was designed not to induce the disturbance waves from downstream of test model. By adjusting choking wedge along forward or backward, it becomes possible to position shock wave at a desired location in the test section. The detailed schematic diagram of flow field to be sketched based on schlieren photographs and driving mechanism of upper wall flat plate are illustrated in **Fig. 3**. The test model used is a two-dimensional Laval nozzle bottom and movable flat upper wall. The nozzle was designed with accuracy not to cause flow separation induced by a pressure gradient in absence of shock wave[17]. Its design

Mach number is 2.0 at nozzle exit section and channel height at the minimum area cross section (**throat**) is 18 mm, the cross section area ratio of nozzle exit to throat is about 1.7. The upper wall is consisted of two parts, one is streamwise movable flat plate with 5 pressure holes along centerline of flat plate and the other is rotatable brass plug with 10 pressure holes. For measurements of spanwise wall pressure distributions, the rotatable plug of brass driven by sliding bevel gear movable along streamwise was used. The upper wall flat in a body of rotatable plug is movable along streamwise by using rack and pinion gear set as seeing in figure. Also, all controlling of stepping motors was accomplished through motor controller and host computer. As a result, it is possible to measure almost continuously the distribution of wall static pressure along streamwise and spanwise by moving the upper wall plate per 1 mm pitch during the tunnel working time. It was ascertained that the movability of upper wall gave no influences on characteristics of global flow fields. By using the movable upper wall flat plate and rotatable plug with multiple pressure holes, the total measurable scopes of wall static pressure along streamwise centerline and spanwise direction are given in **Fig. 4**. Besides, the optical measurable scope is written by using the optical side glass, its full measurable scope is 272 mm. Also the reference coordinate system used in present experiments was described on upper wall plate: x is streamwise displacement along the centerline of upper wall flat plate originated at nozzle throat, x is spanwise direction originated at nozzle throat on centerline of upper wall. At first, the movable upper wall plate on which the practical pressure measurements were performed has multiple pressure holes along streamwise centerline as well as spanwise direction. The upper wall plate whose width in full span is 38 mm and thickness 6 mm is able to move toward upstream and downstream using the rack and pinion gear set as described in **Fig. 3**. By usage of this some confused mechanism, the measurable pressure

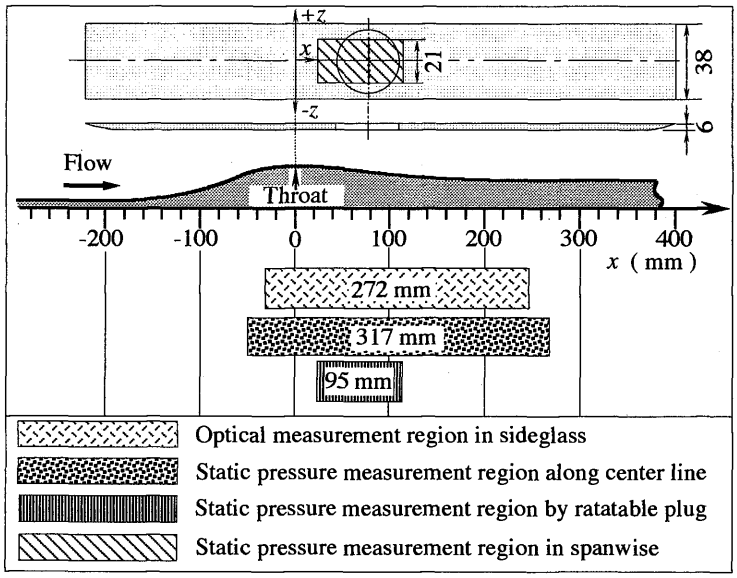

Fig. 4 Wall static pressure and optical measurable scope

scope along x is 317 mm. By using the pressure holes in rotatable plug, its simultaneously measurable scope along both streamwise and spanwise is 95 mm and 21 mm, respectively. Because of structural limitations, the measurable spanwise scope covers about the half of full span, $z/w = -0.55 \sim +0.55$, here $(w/2 = 19)$ is the half width of full span. The mutual setting dimensions of pressure holes on upper wall flat plate containing also rotatable plug is illustrated in **Fig. 5** with all dimensions in millimeter. The spanwise wall pressure measurements were carried out by disposing pressure transducers on rotatable plug along spanwise as seeing in figure. On the other hand, when the experiment related in shock oscillation investigation is carried out, disposing these pressure holes along streamwise supplies spatially wide measurable scope. As described before, by setting the time mean shock position on rotatable plug holes, total 13 pressure transducers along streamwise supply powerful ways to measure mutual correlations using two-points or three-points sampling methods.

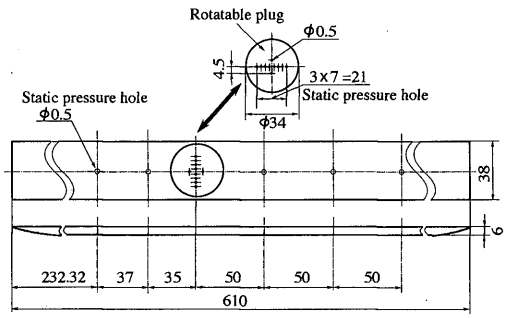

Note : All dimensions in millimeter

Fig. 5 Details of upper wall flat plate and rotatable plug

2. 3 Pressuer transducers

All measurements of wall static pressures in present experiments were made using semi-conduct type pressure transducers with high frequency response characteristics (KULITE XCQ-062-25SG). Detailed installation method and mutual length dimensions of them are illustrated in **Fig. 6** with all dimensions in millimeter. Although, only was depicted the installation in rotatable plug in this figure, the same installation method was applied to upper wall flat plate. The transducer natural frequency quoted by manufacturer is 500 kHz, however, perforated screens protecting the transducers from dust particles limit the effective frequency response to 50 kHz. On the other hand, the influences of pressure transducer size have been investigated by White[18], and recently Schewe[19]. According to their results, in order to detect detailed informations about turbulent fluctuations, usage of transducers as small as possible was recommended. In addition, it was informed that the installation flushness of transducers was very serious factor which influences on the quality of fluctuating surface pressure data by Hanly[20]. He evaluated flushness effects on transducer signal amplitude, power spectral density, coherence and narrow band convection

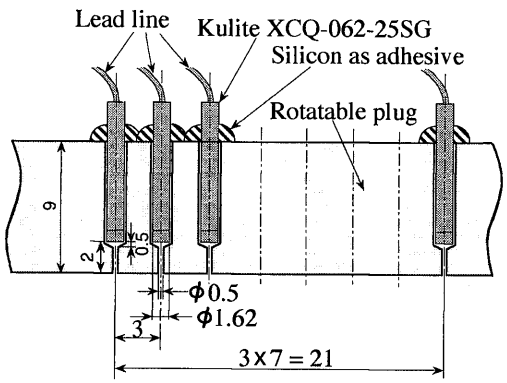

Note : All dimensions in millimeter

Fig. 6 Installation of pressure transducers in rotatable plug

velocity and showed that a very slight protruding of transducer produced adverse effects on the desired pressure fluctuation measurements, whereas a slight submerged transducer produced only small effects. Therefore, instead of being slightly deteriorated its frequency response characteristics, in order to raise spatial resolution effects, dummy drilled holes with 0.5 mm diameter and 2 mm depth were applied in present experiments. The calibration of all transducers were carried out statically referenced to vacuum. According to the results of Raman[21], shock tube tests in dynamic calibration showed a few percent less than those obtained statically. Therefore there are likely to only very small errors due to transducer mounting and calibration.

2. 4 Flow visualization methods

In order to visualize the flow field of STBLI, nominal schlieren method[22] was used. The usage of high quality optical side glass with 10 mm thickness in test section offered useful means of full flow field visualization. The detailed description of an optical axis passed over interaction flow field with density gradient is illustrated in **Fig. 7**. Two kinds of light sources are used: one is electic spark with about three to five microsecond duration, the other is continuous one of xenon (Xe) or tungsten (W) lamp. The latter was applied to take pictures of oscillating shock wave with high clearness. The former was used to adjust light axis, certify the time mean position of shock wave in preliminay test step. On the other hand, a special device is able to be used in order to transform qualitative information of flow visualization as quantitative data. It is Line Image Sensor (Model, EXCEL TECH EYE 1024F) which supplies useful quantitative data. In this case, also is used continuous light source which has uniform brightness. By using the Line Image Sensor, it is possible to take measurements of instantaneous shock position, frequency and amplitude of oscillating shock wave. The detailed results using this device were informed in reference[23]. Additionally, if necessary, Charge Coupled Device (CCD) camera also is used to take informations of flow visualization.

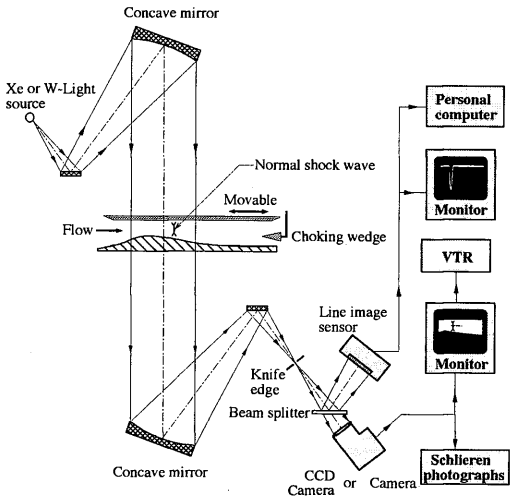

Fig. 7 Schematic diagram of flow visualization

3. Experimental Results and Discussions

3. 1 Test conditions and surveys of boundary layer

The stagnation pressure and temperature in the reservoir tank were always monitored and maintained nearly constant by 101.3 kPa and 288.15 K, respectively during the test. In order to minimize the effect of heat transfer at the wall of test model, the wind tunnel was cooled by operating the tunnel for about one minute before the first test. Under these conditions, the flow Mach numbers at just upstream shock wave calculated by the results of

wall pressure measurements using isentropic relations are ranged about 1.10 to 1.80. According to its range of Mach number, the variation of unit Reynolds number (Re/m) is ranged to about $1.56 \sim 1.32 \times 10^6$, respectively. The boundary layers developing along the test surface were naturally transitioned at far upstream, no any attempt for boundary layer trip was applied. As reported in reference 24, the measurement results of boundary layer thickness using LDV and schlieren photographs showed almost same value within a few percent error, the measurements of boundary layer thickness in present experiment were estimated from schlieren photographs. As described before, the upstream boundary layer thickness were changeable using adjustable upstream duct length: in case of Test I, at nozzle throat $x = 0$ mm, boundary layer thickness $\delta = 0.8$ mm and at $x = 120$ mm, $\delta = 2.0$ mm and in case of Test II, $\delta = 1.0$ mm and $\delta = 2.2$ mm at respective measurement points. In the region of this x direction, the increase of boundary layer thickness δ varies almost linearly and its increase rate is $d\delta/dx = 0.01$.

3. 2 Spanwise pressure measurements

Fig. 8 indicates one result of wall static pressure measurements in case of Test I using 8 spanwise arranged transducers by moving upper wall flat plate along streamwise direction x. The Mach number just upstream shock wave, 1.24 was estimated at $z/w = 0.08$ using minimum wall static pressure and isentropic relation. The value of spanwise axis is normalized to the half of full span width $(w/2)$, also each numbers indicate the dimensionless setting position of 8 pressure transducers, respectively. The classification of normalized wall pressure to stagnation pressure (atmospheric) is given in legend below section of figure. Considering time mean shock position ascertained from schlieren photographs is about 35 mm, this figure shows the spanwise pressure distribution in upstream, interaction itself and downstream region of STBLI. As is evident from this result, the pressure distribution of full flow fields is axisymmetry on spanwise direction. Although, all results of experiments are not proposed in present paper, all results of another test cases and Mach numbers show similar tendencies like this. In order to investigate the influences of upstream boundary layer thickness on STBLI, the pressure measurement results of Test I and Test II at almost on centerline $(z/w = 0.08)$ are illustrated in **Fig. 9**. Mach numbers chosen at just upstream shock wave are 1.24 and 1.60 corresponding to unseparated flow and well-separated flow, respectively[15]. The results of Test I and Test II are marked in open symbols and closed symbols, respectively. In addition, time mean shock positions in each test cases taken from schlieren photographs are marked by white-head arrows and black-head arrows. As known from this figure, the result of $M_1 = 1.24$ shows no remarkable differences, however, that of $M_1 = 1.60$ shows a little differences, near

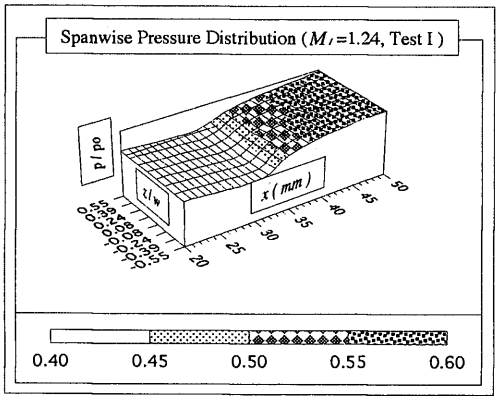

Fig. 8 Wall static pressure distribution of spanwise and streamwise

STBLI region. This fact is the mirror of more complicated interaction behavior containing boundary layer separation bubble motion than that of unseparated flow case. Additionally, the downstream pressure recovery of $M_1 = 1.60$ is somewhat different from that of $M_1 = 1.24$: lower downstream pressure recovery is caused by thick boundary layer[24]. **Fig. 10** illustrates spanwise wall static pressure variations in case of Test I and equal Mach numbers in **Fig. 9**. In each cases, really were acquired total 8 spanwise pressure distributions, however, two of them were illustrated in this figure as a representative. One is the case of $z/w = 0.08$ almost centerline of spanwise (**on-centerline**), the other is $z/w = 0.55$ named "**off-centerline**". The abscissa, $(x-x_s)$ indicates the distance from normal shock section to optional upstream and downstream. This supplies a good information, say, "***upstream influence region***" which is expressed as the upstream distance caused by sudden increase of wall static pressure as evidence of STBLI commencement. As increas of Mach number, the upstream influence region becomes longer than that of lower Mach number. More detailed discussions about this will be required more investigation from now. As evident from this figure, it is obvious that there is pressure difference between the results of on-centerline and off-centerline in case of $M_1 = 1.24$, however, in case of well-separated flow ($M_1 = 1.60$), prominent differences are not found. The reason is able to be explained as following: in case of well separated flow, the fact that there is no conspicuous pressure difference along spanwise must be caused by the large separation bubble developed through full spanwise. Concludingly the uniform flow in well-developed separation bubble along streamwise as well as spanwise shows no great pressure difference.

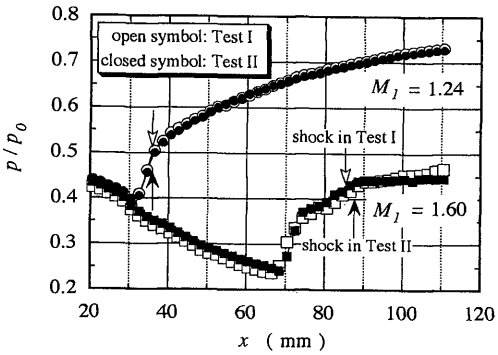

Fig. 9 Effects of upstream boundary layer thickness variation on STBLI

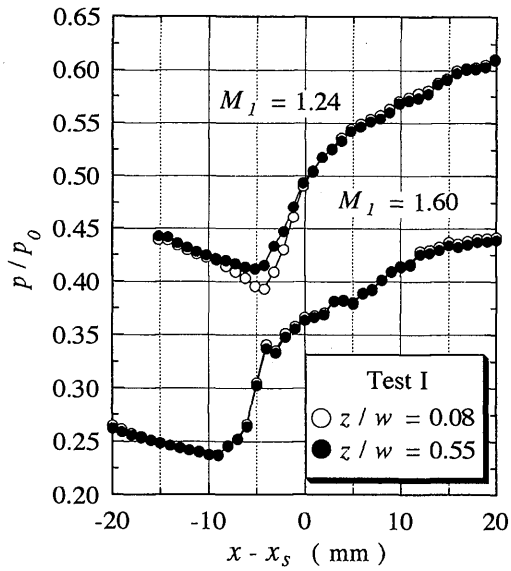

Fig. 10 Variation of spanwise pressure distribution and upstream influece length

4. Conclusions

The detailed spanwise wall static pressure measurements of interaction flow fields induced by weak normal shock wave and turbulent boundary layer were carried out using

two-dimensional nozzle flow. The results of experimental investigation can be summarized as following:

(1) By measuring the spanwise wall static pressure distribution in STBLI region, the flow symmetry to spanwise is clarified in both unseparated and well-separated flow case.

(2) As increase of upstream boundary layer thickness, the pressure distribution of unseparated flow shows no remarkable difference, however, in case of well-separated flow, there is some detectable pressure difference near interaction region and far downstream-its pressure recovery in downstream shows lower level than that of flow with thin boundary layer.

(3) Results of spanwise wall pressure measurements show somewhat large pressure difference in unseparated flow, however, in well-separated flow case is not found its difference that may be caused by well-developed separation bubble.

References

1) Knight, D. D., Improved Calculation of High Speed Inlet Flows: Part Ⅱ Results, AIAA Journal, Vol. 19, No. 2, Feb. (1981), p. 172.

2) Mabey, D. G., Beyond the Buffet Boundary, Aeronautical Journal, Vol. 77, April (1973), p. 201.

3) Kerrobrock, J. L., Flow in Transonic Compressors, AIAA Journal, Vol. 19, No. 1, Jan. (1981), p. 4.

4) Ishiguro, T., Takaki, R., Mitani, T. and Hiraiwa, T., Three-Dimensional Analysis of Scramjet Nozzle Flows, Journal of Propulsion and Power, Vol. 10, No. 4, July-Aug. (1994), p. 540.

5) Sajben, M. and Kroutil, J. C., Effects of Approach Boundary-Layer Thickness on Oscillating, Transonic Diffuser Flows Including a Shock, MDRL Report No, 80-2, (1980).

6) Tan, D. K. M., Tran, T. T. and Bogdonoff, S. M., Wall Pressure Fluctuations in a Three-Dimensional Shock-Wave/Turbulent Boundary Interaction, AIAA Journal, Vol. 25, No. 1, Jan. (1987), p. 14.

7) Brown, J. D., Brown, J. L., Kussoy, M. I., Molt, M. and Horstman, C. C., Two-Component LDV Investigation of Three-Dimensional Shock/Turbulent Boundary-Layer Interactions, AIAA Journal, Vol. 26, No. 1, Jan (1988), p. 52.

8) Davis, D. O., Gessener, F. B. and Kerlick, G. D., Experimental and Numerical Investigation of Supersonic Turbulent Flow Through a Square Duct, AIAA Journal, Vol. 24, No. 9, Sep. (1986), p. 1508.

9) Cambier, L. and Escande, B., Calculation of a Three-Dimensional Shock Wave-Turbulent Boundary-Layer Interaction, AIAA Journal, Vol. 28, No. 11, Nov. (1990), p. 1901.

10) Muck, K. C., Andreopoulos, J. and Dussage, J. P., Unsteady Nature of Shock-Wave/Turbulent Boundary-Layer Interaction, AIAA Journal, Vol. 26, No. 2, Feb. (1988), p. 179.

11) Erengil, M. E. and Dolling, D. S., Correlation of Separation Shock Motion with Pressure Fluctuations in the Incoming Boundary Layer, AIAA Journal, Vol. 29, No. 11, Nov. (1991). p. 1868.

12) Reda, D. C. and Murphy, J. D., Shock Wave/Turbulent Boundary-Layer Interactions in Rectangular Channels, AIAA Journal, Vol. 11, No. 2, Feb. (1973), p. 139.

13) Reda, D. C. and Murphy, J. D., Shock Wave-Turbulent Boundary-Layer Interactions in Rectangula Channels, Part Ⅱ: The Influence of Side Wall Boundary Layers on Incipient Separation and Scale of the Interaction, AIAA Paper No. 73-234, (1973).

14) Reda, D. C. and Murphy, J. D., Sidewall Boundary-Layer Influence on Shock Wave/Turbulent Boundary-Layer Interactions, AIAA Journal, Vol. 11, No. 10, Oct. (1973), p. 1367.

15) Matsuo, K., Hong, J. W., Kim, H. D. and Miyazato, Y., Weak Normal Shock Wave/Turbulent Boundary Layer Interaction in a Supersonic Nozzle: 1st Report, Time-mean Flow Characteristics, Transactions of the Japan Society of Meachanical Engineers, PartB, Vol. 61, No. 581, Jan. (1995), p. 42 (in Japanese).

16) Matsuo, K., Hong, J. W., Kim, H. D. and Miyazato, Y., Weak Normal Shock Wave/Turbulent Boundary Layer Interaction in a Supersonic Nozzle: 2nd Report, Flow Oscillation Characteristics, To be published in Transactions of the Japan Society of Mechanical Engineers, (in Japanese).

17) Tucker, M., Approximate Calculation of Turbulent Boundary-Layer Development in Compressible Flow, NACA Technical Note No. 2337 (1951).

18) White, P. H., Effect of Transducer Size, Shape and Surface Sensitivity on the Measurement of Boundary Layer Pressure, The Journal of Acoustical Society of America, Vol. 41, No. 5 (1967), p. 1358.

19) Schewe, G., On the Structure and Resolution of Wall-Pressure Fluctuations Associated with Turbulent Boundary-Layer Flow, Journal of Fluid Mechanics, Vol. 134 (1983), p. 311.

20) Hanly, R. D., Effects of Transducer Flushness on Fluctuating Surface Pressure Measurements, AIAA Paper No. 75-534, March (1975).

21) Raman, K. R., A Study of Surface Pressure Fluctuations in Hypersonic Turbulent Boundary Layers, NASA CR-2386 (1974).

22) Saad, M. A., *Compressible Fluid Flow*, 2nd edition, Prentice-Hall, (1985), p. 637.

23) Matsuo, K. and Kim, H. D., Measurement of Oscillating Shock Wave in Supersonic Nozzle, Proceedings of the Sixth International Symposium on Flow Visualization, Springer-Verlag, Yokohama, Japan, October 5-9 (1992), p. 612.

24) Carroll, B. F. and Dutton, J. C., Characteristics of Multiple Shock Wave/Turbulent Boundary-Layer Interactions in Rectangular Ducts, Journal of Propulsion and Power, Vol. 6, No. 2, Mar.-Apr. (1990), p. 186.